Broadband wide-view Pancharatnam–Berry phase deflector

JUNYU ZOU,[1,2] **TAO ZHAN,**[1,2] **JIANGHAO XIONG,**[1] **AND SHIN-TSON WU**[1,*]

[1]*College of Optics and Photonics, University of Central Florida, Orlando, Florida 32816, USA*
[2]*These authors contributed equally to this work*
swu@creol.ucf.edu

Abstract: We demonstrate a high-efficiency achromatic, wide-view Pancharatnam–Berry phase deflector (PBD) based on a three-layer multi-twist structure. A practical method to measure the thickness and twist angle of liquid crystal (LC) polymer films is developed based on Jones matrix of twist-nematic liquid crystals. With the help of this new measurement method, we fabricated a three-layer multi-twist PBD. The imaging performance and the angular response of the achromatic wide-view PBD are also characterized. Potential application of PBD for near-eye displays is foreseeable.

1. Introduction

Polarization grating is a device modulating the polarization state of an incident light in angular dimension, and it can separate the incident light into two outgoing beams with orthogonal polarization states [1,2]. Right-handed circularly polarized light (RCP) and left-handed circularly polarized light (LCP) are two polarization eigenstates, if such a grating is fabricated by polarization holography based on continuous Pancharatnam–Berry (PB) phase changing in one dimension [3–6]. In this case, the polarization grating is also called as PB deflector (PBD), which can achieve polarization selectivity with high efficiency and compact size. Recently, PBDs have found widespread applications in astronomy, telecommunication, beam steering, and near-eye displays such as foveated imaging and resolution enhancement [7–11].

A PBD can be regarded as a patterned half-wave plate (HWP), whose operation principle can be explained by following Jones matrix [12]:

$$J'_\pm = \frac{1}{\sqrt{2}} \begin{bmatrix} \cos 2\phi & \sin 2\phi \\ \sin 2\phi & -\cos 2\phi \end{bmatrix} \begin{bmatrix} 1 \\ \pm i \end{bmatrix} = \frac{1}{\sqrt{2}} \begin{bmatrix} 1 \\ \mp i \end{bmatrix} e^{\pm 2i\phi}. \tag{1}$$

For a LCP input light, the output changes to RCP with an extra phase 2ϕ, where ϕ is the azimuthal angle. Once the HWP is patterned with grating profile, then the azimuthal angle will be a linear function along the direction of grating wave vector. This also achieves continuous phase change without introducing discontinuity at the boundary of 2π and 0 modulation as in conventional diffractive optics.

Liquid crystal (LC) exhibits some interesting properties, such as optical and dielectric anisotropies, self-assembly, and the directors can be reoriented by an external field. These properties make LC an outstanding candidate for fabricating patterned HWP using photo-alignment technique [12,13]. In order to create the desired LC orientation pattern, different methods have been developed, including direct writing [14], projection lithography [15] and interference exposure [12]. Direct writing and projection lithography could achieve high resolution patterning, but are time consuming for large-size fabrication. Here in this paper, we fabricate PBDs by the interference of RCP and LCP beams on a photo-alignment layer, which in turn replicates the alignment to the over-coated LC layer.

2.   Device design

In most applications, PBDs with high diffraction efficiency, broad spectral bandwidth, and wide acceptance angle are highly desirable. Taking the advantage of self-aligning property of LC, broadband retardation control with a compact form factor based on multi-twist structure has been demonstrated [16]. Dual-twist achromatic PBD shows a much broader spectral bandwidth than the single-layer non-twist PBD [17], but its angular response is worse, as discussed in [18]. Very recently, biaxial polymeric LC film is employed to widen the angular response of PBD, but the broadband performance has not been achieved yet [19]. Here, we propose a three-layer multi-twist grating structure, which can achieve high efficiency in the visible spectral range and large incident angle. The device structure is shown in Fig. 1. We apply the rigorous coupled-wave analysis method [20,21] to simulate the three layer multi-twist grating structure. In the optimization, the grating period was fixed. The thickness of each layer was set from 0 to 3 μm, and the twist angle of each layer was set from -2π to 2π. Four optimization algorithms, genetic algorithm, particle swarm optimization, adaptive simulated annealing and differential evolution, are interchangeably used to optimize the grating parameters. The optimization results show the thickness of the three LC layers is d_1=0.9 μm, d_2=1.32 μm and d_3=0.88 μm, and the corresponding twist angle is ϕ_1= $-69.4°$, ϕ_2=3.7° and ϕ_3=64°, respectively.
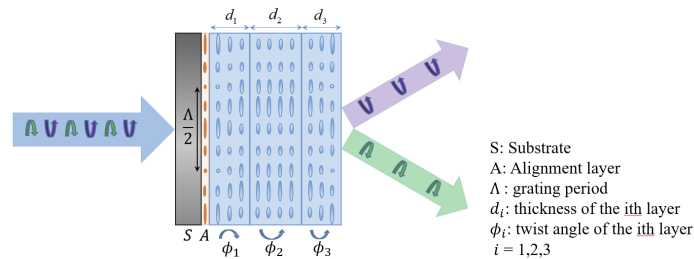

Fig. 1. Three-layer multi-twist PBD structure

3.   Experiment

In this section, a new method to measure the thickness and twist angle of reactive mesogen is developed. High precision thickness and twist angle control play an important role to the performance of our three-layer multi-twist PBD.

3.1.   Thickness and twist angle measurement

During the fabrication of broadband wide-view polarization grating, a key factor is to precisely control the thickness and twist angle of each layer. The film thickness can be measured by a profilometer or atomic force microscope, however, these contact approaches could damage the surface of the polymer film. To overcome this problem, we develop a new method to measure the thickness and twist angle of the polymer film without mechanical engraving. The measurement system setup is shown in Fig. 2(a). The sample is sandwiched between two parallel linear polarizers. The white light source is a broadband halogen lamp.

The structure can be seen as a 0° transmissive twist-nematic (TN) cell. Similar to a transmissive 90° TN cell [22], the transmittance of our device structure can be derived by Jones matrix method as:

$$T_{//} = (\frac{\Phi}{X} \sin \Phi \sin X + \cos \Phi \cos X)^2 + [\frac{\Gamma}{2} \frac{\sin X}{X} \cos(\Phi - 2\beta)]^2, \tag{2}$$
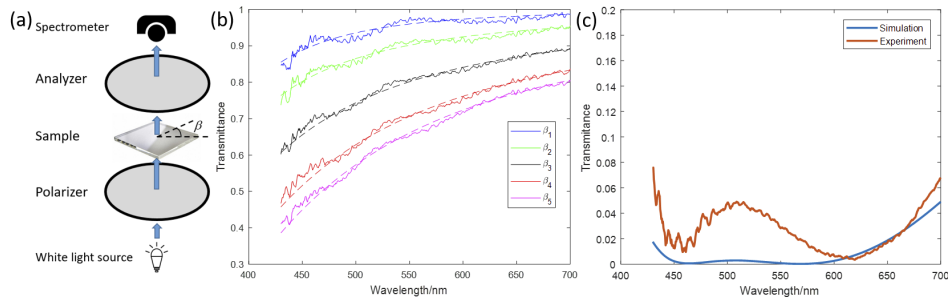
Fig. 2. (a) LC film thickness and twist angle measurement setup, (b) measured and fitted transmission spectra at five β angles for first layer measurement, and (c) comparison between simulation and experiment for three layer structure testing.

where Φ is the twist angle, β is the angle between the polarization axis and the front LC director, Γ is the retardation angle, and $\Gamma = 2\pi d \Delta n / \lambda$, in which d is the LC film thickness, Δn is the LC birefringence, λ is the input light wavelength, and $X = [\phi^2 + (\Gamma/2)^2]^{1/2}$.

When using a broadband white light source as input, the output spectrum is wavelength dependent. By using a spectrometer, the transmission spectrum $T_\parallel(\lambda; \beta, \Phi, d)$ can be recorded, in which λ is the scanning wavelength, while β, Φ, and d are the fitting parameters. In order to make the fitting process more robust, we change the sample orientation four times with $10°$ step, so that five transmission spectra $T_\parallel(\lambda; \beta + 10° \times i, \Phi, d)$ ($i = 0, 1, 2, 3, 4$) are recorded. During the fitting process, we use all the five recorded transmission spectra, so that the error caused by the external parameter β which depends on how we orient the sample, can be reduced and more accurate fitting can be achieved for the internal parameters Φ and d, which depend on the LC film structure. The fitting results are shown in Fig. 2(b), whose average fitting error is less than 1%. The fitted twist angle Φ is $-70.2°$ and thickness d is 0.901 μm. In comparison with the designed parameters ($\Phi_1 = -69.4°$ and $d_1 = 0.90$ μm), the agreement is good.

In order to test the thickness and twist angle of the three-layer multi-twist LC film, we still apply the system structure shown in Fig. 2(a), but the linear polarizer and analyzer are replaced by two left-handed circular polarizers. If the sample is an ideal PBD, then all the incident LCP should be converted to RCP and blocked by the analyzer. Thus, the lower the transmission, the higher the efficiency of PBD. In Fig. 2(c), the three layer test result is targeted to the structure we designed. As Fig. 2(c) depicts, the maximum difference between simulation and experiment is less than 6% in the 430-700 nm range, which means our measurement method is reliable and the three-layer structure meets our design target.

3.2. *Multi-twist PBD fabrication*

In experiment, we fabricated a three-layer multi-twist PBD. In order to form the grating pattern, photo-alignment method was adopted. A thin photo-alignment layer was spin-coated on the glass substrate. The photo-alignment layer consists of brilliant yellow and dimethyl-formamide (DMF). The ratio and the spin speed are listed in Table 1. After the spin-coating process, the alignment layer was exposed under the polarization holography setup depicted in Fig. 3. The setup is a Mach-Zehnder (MZ) interferometer, but one beam directly passing through two polarizing beam splitters without reflection, while the other is reflected by two polarizing beam splitters and two mirrors. With this modification, it is easier to build the MZ interferometer, because only one beam demands fine alignment. In the setup, a collimated laser beam ($\lambda = 457$nm) is split into two orthogonal components by the first polarizing beam splitter (PBS). TM component transmits through the PBS while TE component is reflected. The ratio between TE and TM components can be adjusted by a HWP, which is placed after the laser source. The orientation of dielectric

mirror M_3 can be adjusted to introduce linear phase difference between two optical paths along x axis. The second PBS combines two beams and then makes the two optical paths merging together at the position where the substrate locates. Between the second PBS and substrate, there is a quarter-wave plate (QWP), whose purpose is to convert the two linearly polarized beams to LCP and RCP, respectively. In order to get good pattern exposure, the intensity of LCP and RCP should remain the same at the front surface of the substrate. The photo-alignment layer was exposed to the laser output at 15 mW/cm^2 for 20 min to get the designed grating pattern.
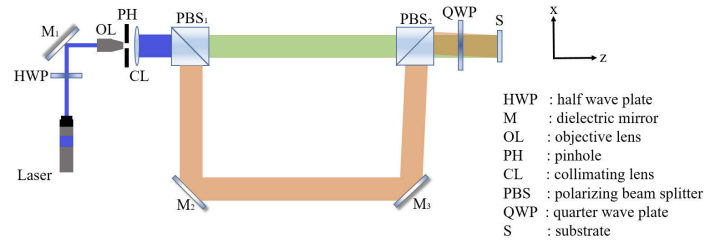

HWP : half wave plate
M : dielectric mirror
OL : objective lens
PH : pinhole
CL : collimating lens
PBS : polarizing beam splitter
QWP : quarter wave plate
S : substrate

Fig. 3. Polarization holography setup for grating pattern exposure.

Table 1. Coating speed and materials for three-layer PBD fabrication

	Solute	Solvent	Solute : Solvent	Coating Speed
Alignment layer	Brilliant Yellow	Dimethyformamide (DMF)	~1:250	500(5s) + 3000(30s)
1st layer	RM257 (95.2%) Irgacure 651 (2.10%) Zonyl 8857A (0.92%) S811 (1.79%)	Tolune	~1:4.81	2450(30s)
2nd layer	RM257 (96.9%) Irgacure 651 (2.18%) Zonyl 8857A (0.955%)	Tolune	~1:3.89	800(5s) + 3000(30s)
3rd layer	RM257 (95.4%) Irgacure 651 (1.39%) Zonyl 8857A (0.948%) R811 (1.68%)	Tolune	~1:3.82	700(5s) + 3000(30s)

According to simulation, the targeted thickness of each layer is 0.9 μm, 1.32 μm and 0.88 μm, and the corresponding twist angle is $-69.4°$, 3.7° and 64°. In order to obtain these targeted values, we spin-coated three layers of reactive mesogen mixture (RMM) onto the substrate. After spin coating of each layer, UV photo-polymerization process was applied to form stabilized polymer film. The components in the RMM include reactive mesogen RM257 (from LC Matter), photo-initiator Irgacure 651 (from BASF), surfactant Zonyl 8857A (from DuPont), and chiral S811/R811 (from HCCH). The ratio of each components and spin speed are shown in Table 1. For the second layer, the twist angle is very small. Moreover, in experiment we found that the LC molecules would not twist when the chiral concentration was too low. Therefore, we did not add any chiral to the second layer so that the twist angle of second layer was zero. This would bring negligible error to the efficiency performance according to our simulation.

4. Results and Discussion

Figure 4(a) shows the image of PBD through a polarization microscope (Olympus BX51). The grating structure is clearly observed. The grating period was set to a relatively large value, ~35

μm, rendering the grating in the Raman-Nath regime. Under normal incidence, the deflection angle is 0.75°, 0.87° and 1° at 457nm, 532nm and 635nm, respectively. This kind of long-period polarization-dependent grating is very useful for resolution enhancement in near-eye displays [11]. We took a picture for testing with this PBD placed between the camera and a keyboard. The input image is shown in Fig. 4(b) and the output image after the PBD is shown in Fig. 4(c). The input is unpolarized ambient light, consisting of 50% RCP and 50% LCP. In Fig. 4(c), two ± 1st order diffracted lights are clearly observed. The zero order leakage is negligible, which means the PBD has nearly 100% diffraction efficiency in the visible spectral region. The PBD splits the input beam into two outgoing beams, so that the brightness of each order is reduced to ~50%. However, the transmittance is very high and the grating area is clear. We can see a little yellowish color of the white alphabets in the output image. This is because the alignment layer material (Brilliant Yellow) has about 15% absorption in the blue region. There are also other kinds of alignment layer materials that have negligible absorption to visible light, such as SD1 and PAM-0042 from DIC Corporation. We utilized Brilliant Yellow because it is cost-effective and commercially available.
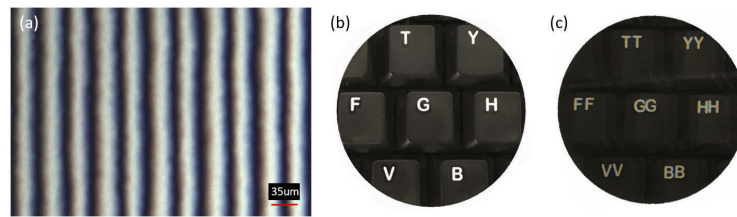

Fig. 4. Imaging results of the fabricated three-layer multi-twist PBD: (a) observed grating structure from a polarization microscope, and imaging performance test (b) input and (c) output.

The first order diffraction efficiency of the PBD was measured at three primary wavelengths: R = 635 nm, G = 532 nm and B = 457 nm. Results are plotted in Fig. 5, which are normalized with the total output power at corresponding incident angle and wavelength, so the influence of absorption and Fresnel reflection are eliminated. At each wavelength, the angular spectrum was measured from − 50° to 50° at 10° interval [Fig. 5(b), (c), (d)]. The experimental results agree with the simulation very well at red and green wavelengths, where the average fitting error is about 2%. The first order diffraction efficiency varies from 92.3% to 98.1% for red
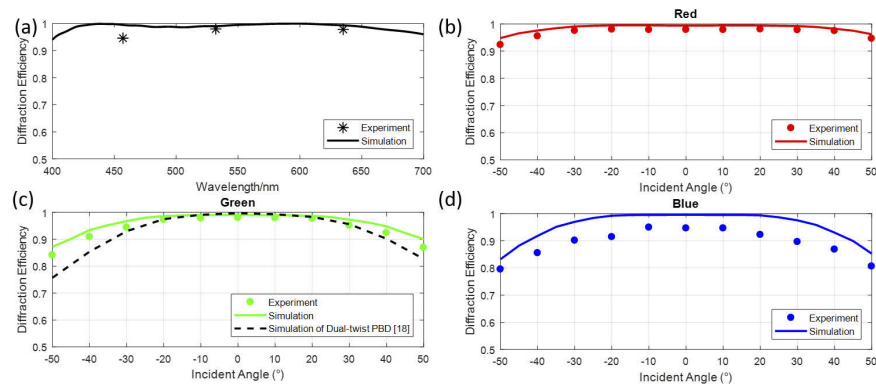

Fig. 5. Simulated and measured (a) spectral response of the three-layer multi-twist PBD and its angular response at (b) Red (c) Green (d) Blue wavelength.

and from 84.1% to 98.0% for green. For blue light, the first order diffraction efficiency varies from 84.1% to 99.5% by simulation, but the experimental result is from 79.5% to 94.9%. The average error is around 5% between simulation and experiment. A possible explanation is that blue light has a larger scattering. By comparing the angular response of dual-twist PBD in Fig. 5(c), the advantage of three-layer multi-twist PBD is significant at large incident angle. For dual-twist PBD, the diffraction efficiency is 75.7% at $-50°$ [18], but the three-layer multi-twist PBD remains at 87.2% in simulation and 84.1% in experiment.

5. Conclusion

We have designed and experimentally demonstrated a high efficiency achromatic wide-view PBD, which consists of three layers of reactive mesogen mixture. The thickness and twist angle of the LC film can be measured precisely by a newly proposed method. Our PBD indeed exhibits broadband and wide angular response. Simulation agrees well with experiment. Widespread application of such PBD for near-eye displays is foreseeable.

Funding

References

1. G. Cincotti, "Polarization gratings: Design and applications," IEEE J. Quantum Electron. **39**(12), 1645–1652 (2003).
2. T. Zhan, Y. H. Lee, G. Tan, J. Xiong, K. Yin, F. Gou, J. Zou, N. Zhang, D. Zhao, J. Yang, S. Liu, and S. T. Wu, "Pancharatnam-Berry optical elements for head-up and near-eye Displays," J. Opt. Soc. Am. B **36**(5), D52–D65 (2019).
3. T. Todorov, L. Nikolova, and N. Tomova, "Polarization holography. 2: Polarization holographic gratings in photoanisotropic materials with and without intrinsic birefringence," Appl. Opt. **23**(24), 4588–4591 (1984).
4. K. Gao, C. McGinty, H. Payson, S. Berry, J. Vornheim, V. Finnemeyer, B. Roberts, and P. Bos, "High-efficiency large-angle Pancharatnam phase deflector based on dual-twist design," Opt. Express **25**(6), 6283–6293 (2017).
5. S. Pancharatnam, "Achromatic combinations of birefringent plates. Part II. An achromatic quarter wave plate," Proc. - Indian Acad. Sci., Sect. A **41**(4), 137–144 (1955).
6. M. V. Berry, "Quantal phase factors accompanying adiabatic changes," Proc. R. Soc. London, Ser. A **392**(1802), 45–57 (1984).
7. C. Packham, M. Escuti, J. Ginn, C. Oh, I. Quijano, and G. Boreman, "Polarization gratings: A novel polarimetric component for astronomical instruments," Publ. Astron. Soc. Pac. **122**(898), 1471–1482 (2010).
8. S. Yeralan, J. Gunther, D. L. Ritums, R. Cid, and M. M. Popovich, "Switchable Bragg grating devices for telecommunications applications," Opt. Eng. **41**(8), 1774–1779 (2002).
9. J. Kim, C. Oh, M. J. Escuti, L. Hosting, and S. Serati, "Wide-angle nonmechanical beam steering using thin liquid crystal polarization gratings," Proc. SPIE **7093**, 709302 (2008).
10. G. Tan, Y. H. Lee, T. Zhan, J. Yang, S. Liu, D. F. Zhao, and S. T. Wu, "Foveated imaging for near-eye displays," Opt. Express **26**(19), 25076–25085 (2018).
11. T. Zhan, J. Xiong, G. Tan, Y. H. Lee, J. Yang, S. Liu, and S. T. Wu, "Improving near-eye display resolution by polarization multiplexing," Opt. Express **27**(11), 15327–15334 (2019).
12. J. Xiong, T. Zhan, and S. T. Wu, "A versatile method for fabricating Pancharatnam-Berry micro-optical elements," Opt. Express **27**(20), 27831–27840 (2019).
13. V. G. Chigrinov, V. M. Kozenkov, and H. S. Kwok, *Photoalignment of Liquid Crystalline Materials: Physics and Applications* (Wiley, 2008).
14. J. Kim, Y. Li, M. N. Miskiewicz, C. Oh, M. W. Kudenov, and M. J. Escuti, "Fabrication of ideal geometric-phase holograms with arbitrary wavefronts," Optica **2**(11), 958–964 (2015).
15. L. De Sio, D. E. Roberts, Z. Liao, S. Nersisyan, O. Uskova, L. Wickboldt, N. Tabiryan, D. M. Steeves, and B. R. Kimball, "Digital polarization holography advancing geometrical phase optics," Opt. Express **24**(16), 18297–18306 (2016).
16. R. K. Komanduri, K. F. Lawler, and M. J. Escuti, "Multi-twist retarders: broadband retardation control using self-aligning reactive liquid crystal layers," Opt. Express **21**(1), 404–420 (2013).
17. C. Oh and M. J. Escuti, "Achromatic diffraction from polarization gratings with high efficiency," Opt. Lett. **33**(20), 2287–2289 (2008).
18. X. Xiang and M. J. Escuti, "Numerical modeling of polarization gratings by rigorous coupled wave analysis"," Proc. SPIE **9769**, 976918 (2016).

19. R. Momosaki, K. Ashikawa, M. Sakamoto, K. Noda, T. Sasaki, N. Kawatsuki, and H. Ono, "Incident angle dependence-reduced polarization grating performance by using optically biaxial polymer liquid crystal," Opt. Lett. **44**(24), 5929–5932 (2019).
20. M. G. Moharam, D. A. Pommet, E. B. Grann, and T. K. Gaylord, "Stable implementation of the rigorous coupled-wave analysis for surface-relief gratings: enhanced transmittance matrix approach," J. Opt. Soc. Am. A **12**(5), 1077–1086 (1995).
21. M. G. Moharam and T. K. Gaylord, "Rigorous coupled-wave analysis of planar-grating diffraction," J. Opt. Soc. Am. A **71**(7), 811–818 (1981).
22. S. T. Wu and D. K. Yang, *Reflective Liquid Crystal Displays* (Wiley, 2001).